Supplementary Information

Tungsten-Based Ternary Catalysts for Selective Growth of Single-Walled Carbon Nanotubes

Jae Hun Hwang[a], Geon Han[b], Young Soo Park[b], Sang Won Lee*[a] and Young Chul Choi*[b,c,d]

a. Industrialization Division, Korea Carbon Industry Promotion Agency (KCARBON), 110-11 Banryong-ro, Deokjin-gu, Jeonju-shi, 54852, Republic of Korea
b. Department of Carbon Convergence and Energy Engineering, Jeonju University, Jeonju, 55069, Republic of Korea
c. Department of Convergence, Jeonju University, Jeonju, 55069, Republic of Korea
d. Department of Advanced Materials and Chemical Engineering, Jeonju University, Jeonju, 55069, Republic of Korea

* Corresponding authors.

E-mail addresses: swonlee00@kcarbon.or.kr(S.W. Lee), youngchoi@jj.ac.kr(Y.C. Choi)

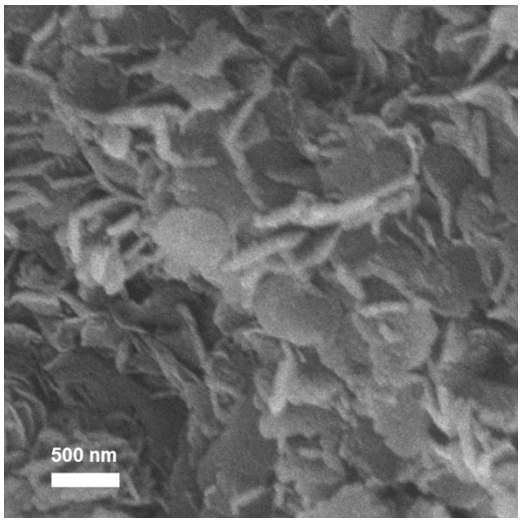

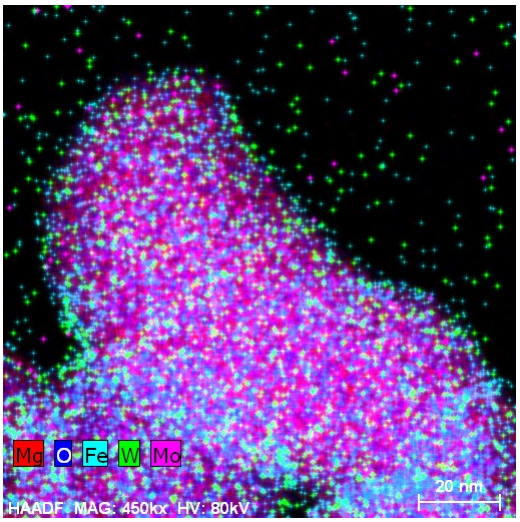

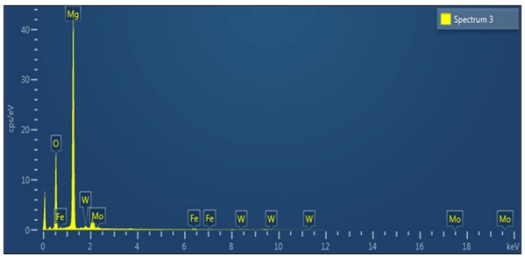

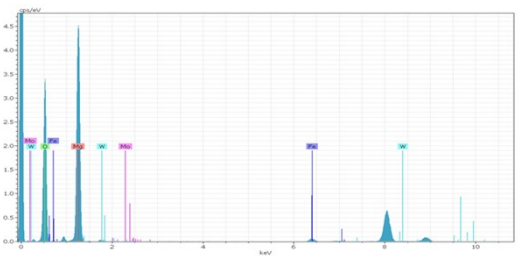

Element	wt. %	wt. % Sigma
O	36.3	0.2
Mg	56.4	0.3
Fe	1.9	0.2
Mo	2.1	0.1
W	3.3	0.2
Total:	100.0	

Element	wt. %	at. %
O	35.68	27.62
Mg	60.89	71.59
Fe	1.60	0.54
Mo	0.60	0.12
W	1.23	0.13
Total:	100.00	100.00

Fig. S1 FESEM-EDS and HRTEM-EDS result of calcinated catalyst. The figure presents the change in the morphology of the MgO impregnated metal catalyst following calcination. It also demonstrates the presence of the metals(FESEM-EDS) and the increased content of oxygen in the catalyst. The elemental composition of the metal catalysts was confirmed by HRTEM–EDS analysis.

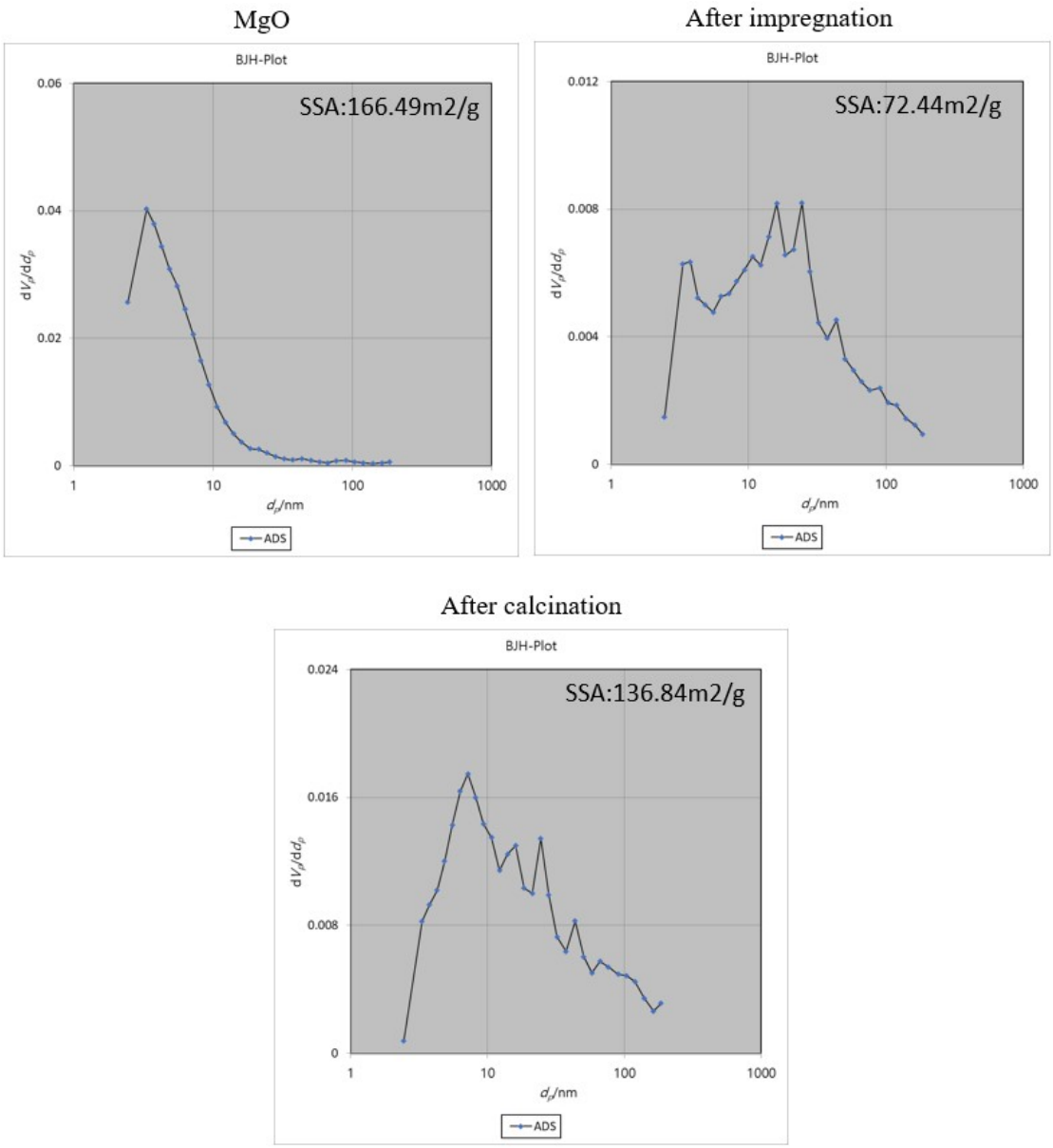

Fig. S2 Barrett-Joyner-Halenda(BJH) plot of MgO, impregnated catalyst and calcined catalyst. The porosity of the mesoporous MgO is reduced due to the impregnation of the metal catalyst within the mesopores. The calcination process leads to alterations in the specific surface area(SSA) and pore distribution, resulting in the formation of alloying and the oxide layer.

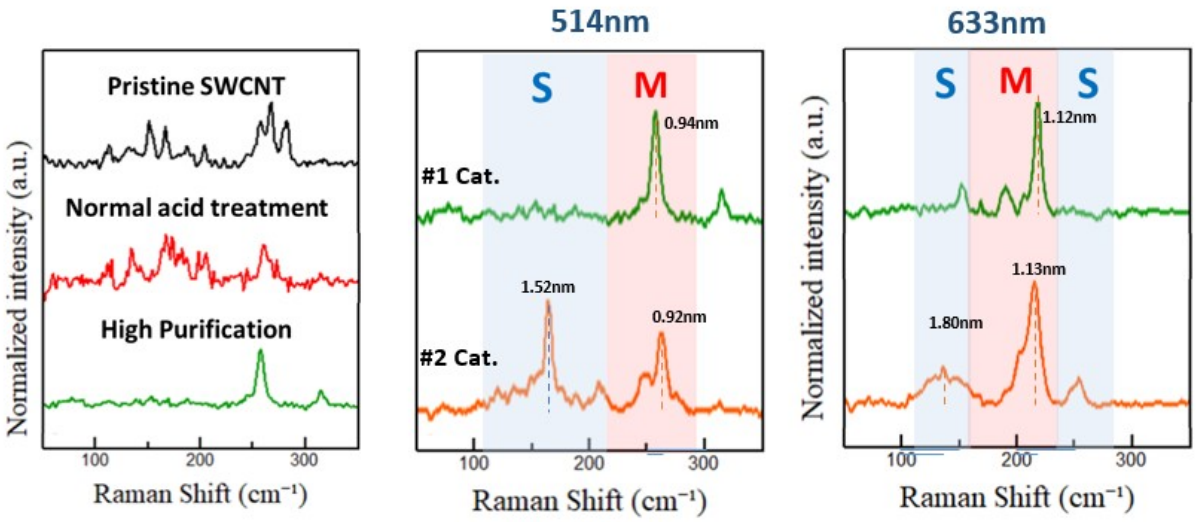

Fig. S3 Raman RBM mode of purified SWCNT. The residual catalyst present at the tip of SWCNTs has the effect of affecting their radial vibrations (RBM). Through a process of high purification to approximately 99% (Figure 4c), the interference in the RBM mode of SWCNTs has been minimized. The RBM signal has been measured at individual tubes through a homogeneous dispersion process using a high pressure homogenizer (this will be published in a forthcoming companion paper).

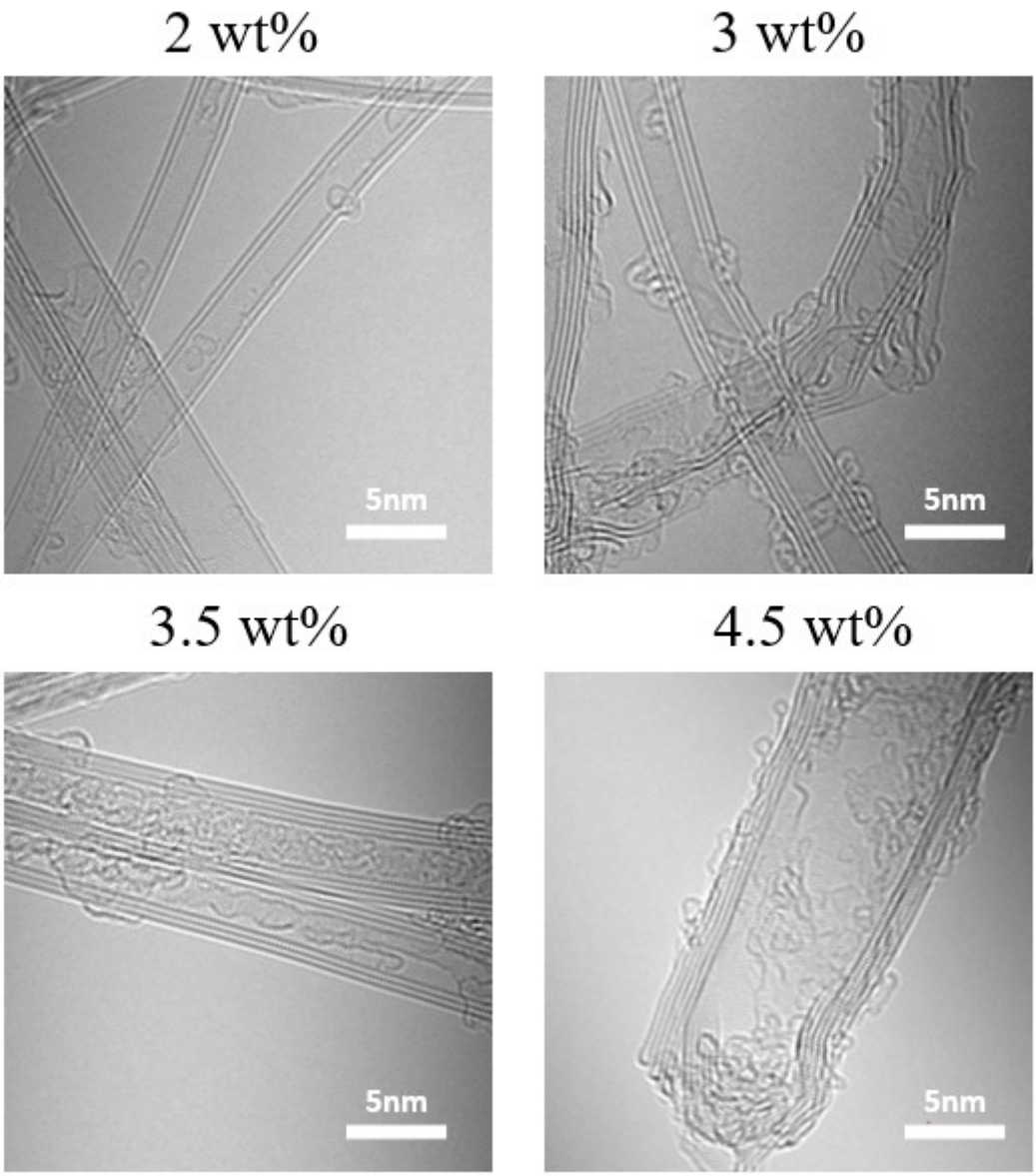

Fig. S4 HRTEM images of CNTs grown on the catalyst as a function of the W content. As the W content of the ternary catalyst for the growth of SWCNTs exceeds 1.5%, there is a substantial increase in both the wall number and diameter. We optimized a W content of 1.5% to control the diameter of SWCNTs and found that a high content of W resulted in the synthesis of large diameter CNTs as a result of the poor dispersibility of the metal catalysts.

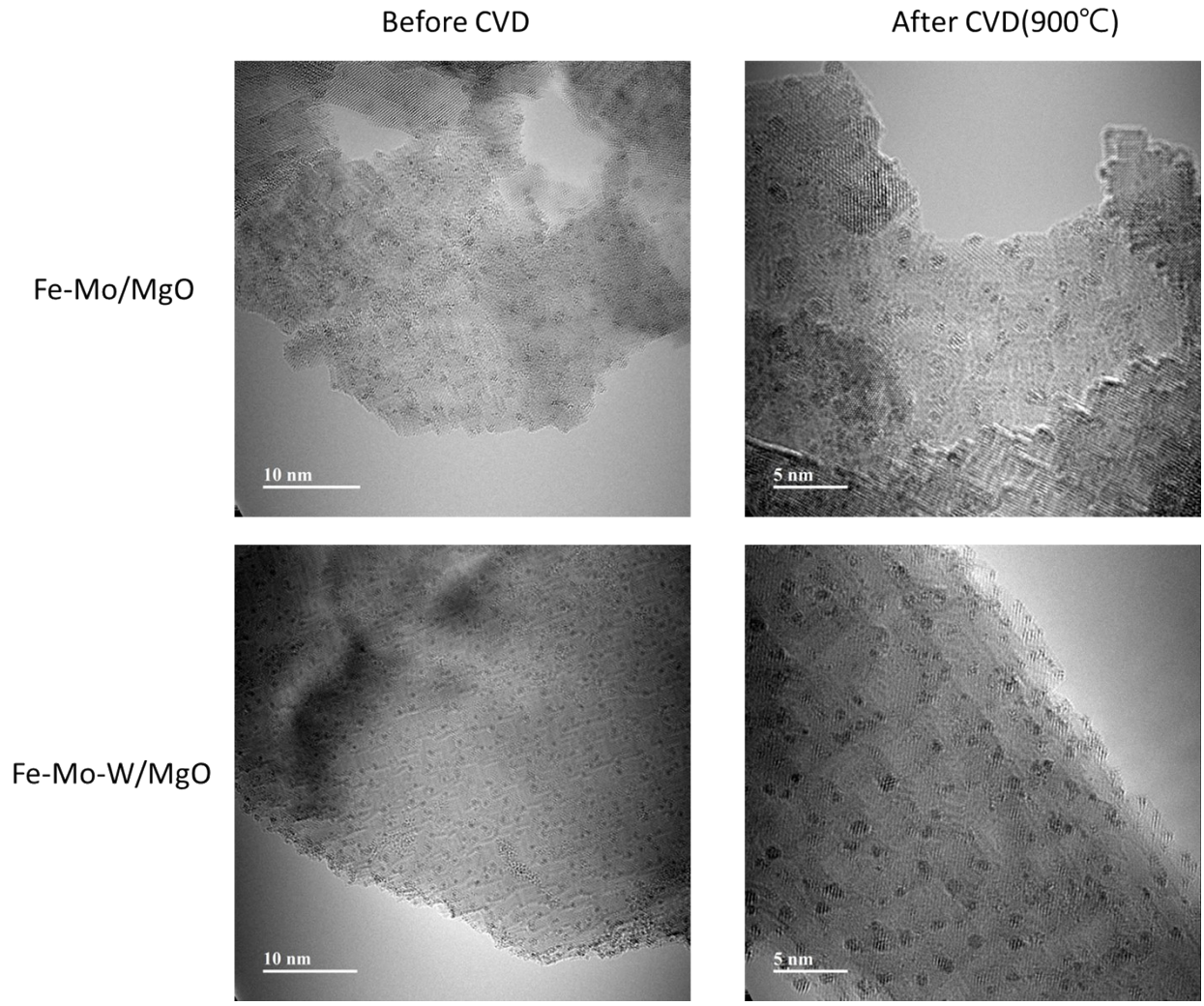

Fig. S5 HRTEM images of Fe–Mo/MgO and Fe–Mo–W/MgO catalysts before and after high-temperature treatment. (a) HR-TEM image of the Fe–Mo/MgO catalyst after calcination. (b) TEM image of the Fe–Mo/MgO catalyst after undergoing a CVD process at 900 °C in the absence of methane, where partially enlarged catalyst particles are observed, indicating a non-uniform particle size distribution after high-temperature exposure. (c) HR-TEM image of the Fe–Mo–W/MgO catalyst after calcination. (d) TEM image of the Fe–Mo–W/MgO catalyst after the CVD process at 900 °C without methane, showing a relatively uniform distribution of catalyst nanoparticles with an average size of approximately 1.2 nm.

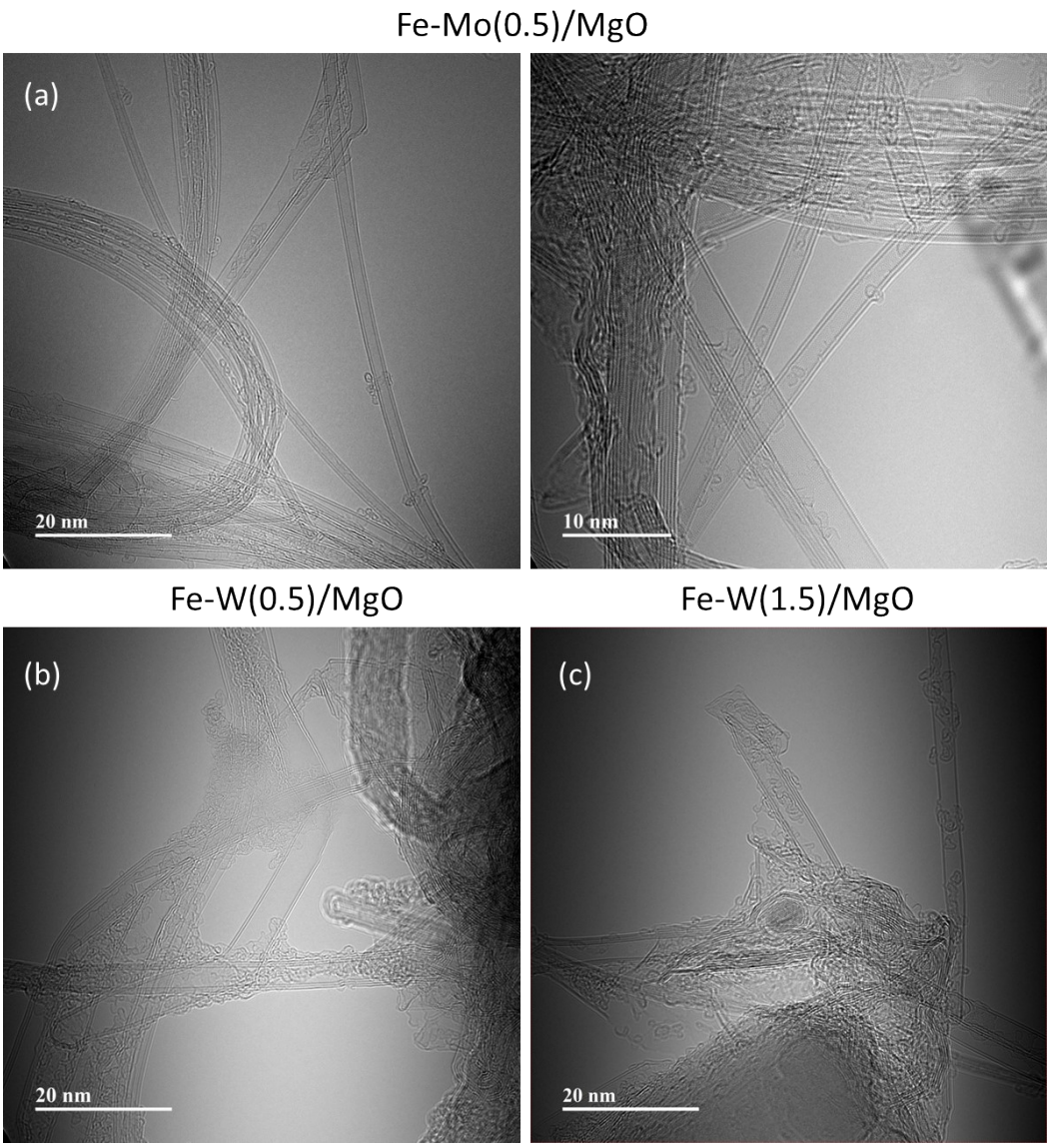

Fig. S6 HRTEM images of carbon nanotubes synthesized using binary catalysts with different metal compositions: (a) Fe–Mo catalyst (Fe:Mo = 1.5:0.5), (b) Fe–W catalyst (Fe:W = 1.5:0.5), and (c) Fe–W catalyst (Fe:W = 1.5:1.5). Differences in tube wall number and diameter distributions are observed depending on the catalyst composition. These images present a direct morphological comparison of CNTs synthesized from the binary catalyst systems.